ANALYSIS OF ADHESIVE BONDING USING DIGITAL IMAGE CORRELATION TECHNIQUE

L.C.S. Nunes, luizcsn@vm.uff.br / luizcn@mec.uff.br
R.A.C. Dias, rodrigoacdias@yahoo.com.br
V.M.F. Nascimento, vitor_marc@yahoo.com.br
Departamento de Engenharia Mecânica – Universidade Federal Fluminense - UFF
Laboratório de Mecânica Teórica e Aplicada - LMTA
Rua Passo da Pátria, 156, Bloco E, Sala 216, Niterói, RJ CEP 24210-240, Tel.: 2629-5588

P.A.M. Santos, pams@if.uff.br
Instituto de Física – Universidade Federal Fluminense - UFF
Laboratório de Óptica Não Linear e Aplicada
Av. Gal Milton Tavares de Souza s/n Gragoatá, Niterói, RJ CEP 24020-005, Tel.: 2629-5767

Abstract. *This paper reports on an investigation relating to full field displacement distribution in a single lap adhesive bonded joint. Experimental analysis is conducted via Digital Image Correlation technique and numerical analysis is done using the finite element technique. Single lap joint subjected to tensile loading represents the simplest form of adhesive joints and is used as a standard test specimen for characterizing adhesive properties and strength. Digital Image Correlation (DIC) is an optical technique developed for full field and non contact measuring of surface displacement and deformation. This technique requires a digital imaging system to record images of the surfaces before and after deformation. The images are then compared using advanced image correlation and processing algorithms in order to determine the displacement and deformation gradients.*

Keywords*: Single lap joint, Full field displacement, DIC technique*

1. INTRODUCTION

The shear lag model, first proposed by O. Volkersen, 1938 (D.A. Dillard, A.V. Pocius, Adhesion Science And Engineering, 2002), is one of the most fundamental concepts in the transfer of load between two members joined by an adhesive. Shear tests are generally carried out for one of two purposes. The first is to compare the performance of adhesives in a joint that is subjected to the most common type of loading, namely, shearing. The second purpose is to determine the actual mechanical response of the adhesive for use in subsequent joint design. In 1944, Goland and Reissner developed a model considering the effects of the adherend bending and the peel stress, as well as the shear stress, in the adhesive layer in a single lap joint. This paper has been widely employed in the 4adhesive stress analysis and it is considered as a classical model which all recent works take it as reference.

Recently, Quantian Luo and Liyong Tong (2007) developed a novel closed-form and accurate solutions for the edge moment factor and adhesive stresses for single lap adhesive bonded joints, and a complementary work based on finite element technique was presented by E. Oterkus *et. al* (2006). Practically, all works present theoretical and numerical analyses, but rarely one experimental analysis.

The aim of this work was to use an experimental technique, know as Digital Image Correlation (DIC) technique, to analyze the single lap joint. The DIC is a non-contact optical technique that allows the full-field estimation of strains on a surface under an applied deformation. One example of application, developed by Nunes *et al*. (2007), takes into account the DIC technique, to generate full field displacement and the Levenberg-Marquardt method to solve associated inverse, to estimate the elasticity modulus of an aluminum beam using a simple experimental setup.

2. CLASSICAL STRESS THEORIES FOR ADHESIVELY BONDED SINGLE LAP JOINTS

The first analysis proposed by Volkersen, was based on a simple shear lag model for load transfer from one adherend to another by a simple shearing mechanism alone. In the model, the adherends are assumed in tension and the adhesive is in shear only, and both are constant across the thickness. Nevertheless, this model does not reflect the effect of the adherend bending and shear deformations.

In this work it is taken into account the following assumptions, based in the basic shear lag model:

- The adherends do not deform in shear, implying that the shear modulus of the adherends is much greater than that of the adhesive.
- Adhesive and adherends are assumed to behave in a linear elastic manner.
- Bonding is assumed to be perfect along both bond planes.
- The effects of the bond terminus are ignored.
- Plane stress conditions are assumed, ignoring complications arising from different Poisson contractions in the bonded region and single adherend regions.

The single lap joint is illustrated schematically in Fig. 1. Considering this geometry and the hypotheses assumed interiorly, the shear stresses cause sliding in an element of material as is shown in Fig. 2.

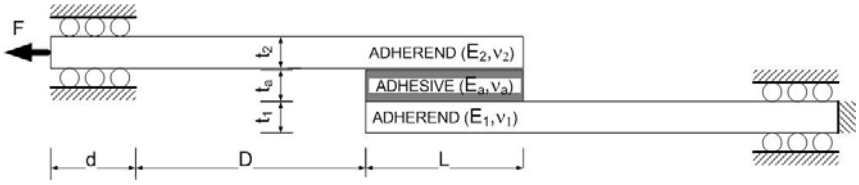

Figure 1. Typical single lap joints.

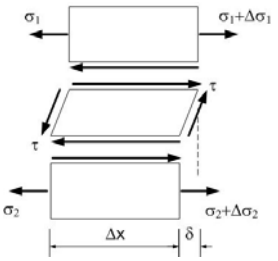

Figure 2. Free-body diagram of an infinitesimal element of a single-lap joint.

Considering the free body diagram of an infinitesimal element of the single lap joint, illustrated in Fig. 2, the equilibrium equations and constitutive relations of adherends can be given as:

$$\frac{\partial \sigma_1}{\partial x} = \frac{\tau}{t_1}, \quad \frac{\partial \sigma_2}{\partial x} = -\frac{\tau}{t_2} \tag{1}$$

The kinematic expressions of adherends are:

$$\frac{\partial \delta}{\partial x} = \varepsilon_1 - \varepsilon_2, \qquad \gamma = \frac{\delta}{t_a} \tag{2}$$

The constitutive relationship, assuming linear elastic behaves, can be express by:

$$\varepsilon_1 = \frac{\sigma_1}{E_1}, \qquad \varepsilon_2 = \frac{\sigma_2}{E_2}, \qquad \gamma = \frac{\tau}{G_a} \tag{3}$$

Taking the derivative with respect to x of Eq. (3) and combining the equations,

$$\frac{\partial \tau}{\partial x} = G_a \frac{\partial \gamma}{\partial x} = \frac{G_a}{t_a}\frac{\partial \delta}{\partial x} = \frac{G_a}{t_a}\left(\varepsilon_1 - \varepsilon_2\right) = \frac{G_a}{t_a}\left(\frac{\sigma_1}{E_1} - \frac{\sigma_2}{E_2}\right) \tag{4}$$

Taking the second derivative of Eq. (8)

$$\frac{\partial^2 \tau}{\partial x^2} = \frac{G_a}{t_a}\left(\frac{1}{E_1}\frac{\partial \sigma_1}{\partial x} - \frac{1}{E_2}\frac{\partial \sigma_2}{\partial x}\right) = \frac{G_a}{t_a}\left(\frac{E_1 t_1 + E_2 t_2}{E_1 t_1 E_2 t_2}\right)\tau \tag{5}$$

The governing differential equation is

$$\frac{\partial^2 \tau}{\partial x^2} - \omega^2 \tau = 0 \text{, where } \omega = \sqrt{\frac{G_a}{t_a}\left(\frac{E_1 t_1 + E_2 t_2}{E_1 t_1 E_2 t_2}\right)} \tag{6}$$

The solution to this differential equation is

$$\tau(x) = A\cosh\omega x + B\sinh\omega x \tag{7}$$

By equation (4), considering ε_1 and ε_2 vanish at the right and left ends of adherends 1 and 2, respectively, the stresses in Eq. (7) are constrained by the following boundary conditions:

$$\left.\frac{d\tau}{dx}\right|_{-L/2} = -\frac{G_a P}{t_a E_2 t_2}, \qquad \left.\frac{d\tau}{dx}\right|_{L/2} = \frac{G_a P}{t_a E_1 t_1} \tag{8}$$

where P is the axial load per unit width of the joint

Then, the final solution for the shear stress in the adhesive layer can be expressed as the following forms:

$$\tau(x) = \frac{P\omega}{2}\left[\frac{\cosh(\omega x)}{\sinh(\omega L/2)} + \left(\frac{E_2 t_2 - E_1 t_1}{E_2 t_2 + E_1 t_1}\right)\frac{\sinh(\omega x)}{\cosh(\omega L/2)}\right] \tag{9}$$

3. DIGITAL IMAGE CORRELATION (DIC) METHOD

The DIC method is an optical-numerical full-field surface displacement measuring technique, which is nowadays widely used in experimental mechanics. This technique is based on a comparison between two images of the specimen coated by a random speckle pattern in the underformed and in the deformed state. Its special merits are non-contact measurement, simple optic setup, no special preparation of specimens and no special illumination.

The basic principle of DIC method is to search for the maximum correlation between small zones in the underformed and deformed images, as illustrated in Figure 1, from which the displacement at different positions in the zone of interest can be obtained. The simplest image-matching procedure is the cross-correlation, which can determine the in plane displacement field (u, v) by matching different zones of two images.

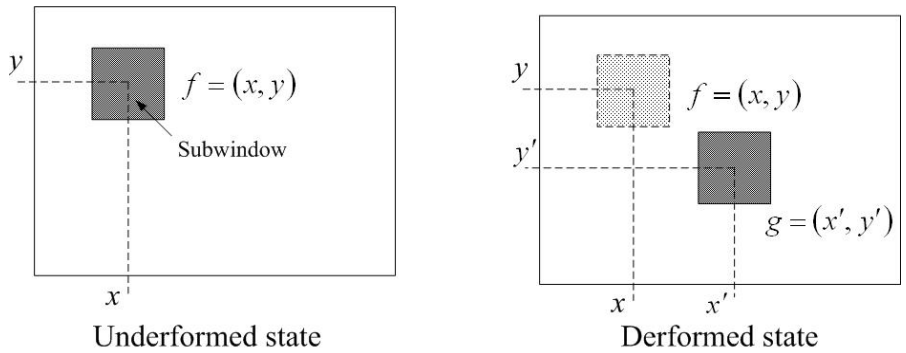

Figure 3. Schematic diagram of the deformation relation.

A commonly used cross-correlation function is defined as below:

$$C(u,v) = \frac{\sum_{i=1}^{m}\sum_{j=1}^{m}\left[f(x_i,y_j)-\bar{f}\right]\left[g(x_i',y_j')-\bar{g}\right]}{\sqrt{\sum_{i=1}^{m}\sum_{j=1}^{m}\left[f(x_i,y_j)-\bar{f}\right]^2}\sqrt{\sum_{i=1}^{m}\sum_{j=1}^{m}\left[g(x_i',y_j')-\bar{g}\right]^2}} \tag{10}$$

where

$$\begin{aligned} x' &= x + u + \frac{\partial u}{\partial x}dx + \frac{\partial u}{\partial y}dy \\ y' &= y + v + \frac{\partial v}{\partial x}dx + \frac{\partial v}{\partial y}dy \end{aligned} \tag{11}$$

$f(x,y)$ is the gray level value at coordinate (x,y) for the underformed or original image and $g(x',y')$ is the gray level value at coordinate (x',y') for deformed or target image, $\bar{f}$ and $\bar{g}$ are the average gray values and u and v are the displacement component for the subset centers in the *x* and *y* directions, respectively.

The camera uses a small rectangular piece of silicon, which has been segmented into H x V array of individual light sensitive cell, also known as pixel. Each pixel store a certain gray scale value ranging from 0 to 255, in accordance with the intensity of the light reflected by the surface of specimen.

Relative to specimen preparation, the aim is to create a speckle pattern on the specimen surface, the smaller the grains, the higher the spatial resolution.

The results will depend on CCD pixel resolution, speckle size and DIC software considered.

4. RESULTS

4.1. Experimental results

The experimental arrangement involves an apparatus developed to apply strain in a single lap joint, a CCD camera set perpendicularly to the specimen and a computer to capture and process the images, as shown in Fig. 4. The single lap joint, fixed in the strain apparatus in agreement with the geometrical model as shown in Fig. 1, was covered with painted speckles (random black and white pattern). Two images of this single lap joint were recorded using the CCD camera, before and after load, with a resolution of 640x480 pixels. In this experimental configuration one pixel of the CCD camera corresponds to an area of about 25.3×25.3 μm on the object.

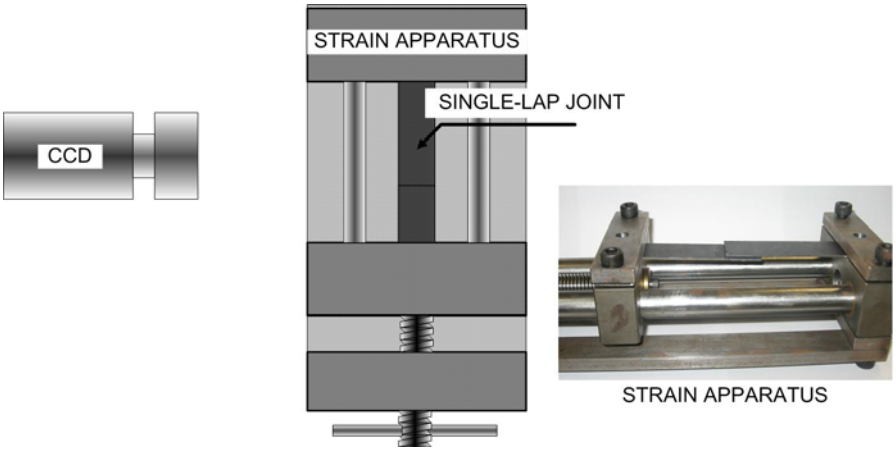

Figure 4. Experimental arrangement with strain apparatus of bonded joint details.

In order to obtain the experimental results, the geometry model for the single lap joint, schematically illustrated in Fig. 1, was considered with the following data: (a) Applied force, F = 45 N; (b) length of restraint against transversal motion, d = 25 mm; segment of length, D = 55 mm; joint length, L = 24 mm; adherend and adhesive thickness, $t_1 = t_2 = 1{,}7$ mm and $t_a = 0.9$ mm, respectively. The upper and lower adherends have the same characteristics and the material proprieties of adherends and adhesive are shown in Tab.1.

Table1. Material Proprieties of adherend and adhesive.

	Material	Modulus of elasticity, E (GPa)	Poisson's ratio, ν
Adherend	Steel A36	207	0.3
Adhesive	Silicone rubber (polydimethylsiloxane)	0.00075	0.5

The two images of the single lap joint cover with painted speckles are taken in the same region, as illustrated in Figure 5, considering two different loads of 0 and 40 N. These images were used to determinate full-field displacement by means of computer software based on correlation theory, presented in item 3. This software has been developed in our laboratory.

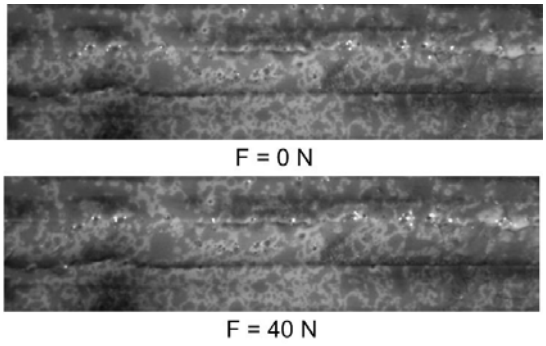

Figure 5. Pattern of coating specimen underformed and deformed.

The results of full field displacement u(x,y), associated with x direction, are shown in Fig. 6 and Fig. 7. These results are based on two images record for different load, as shown in Fig. 5. It is clear to observe the shear comportment of the silicone rubber. In this case, the Young' modulus of adherend is larger that adhesive, i.e., the deformation in the adherend is neglected and the effect of bending too.

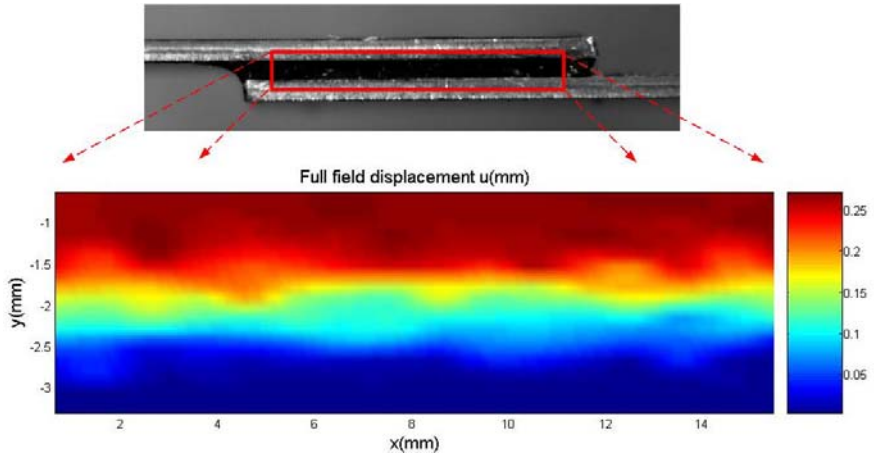

Figure 6. Full field displacement u(x,y), associated with x direction. Color map.

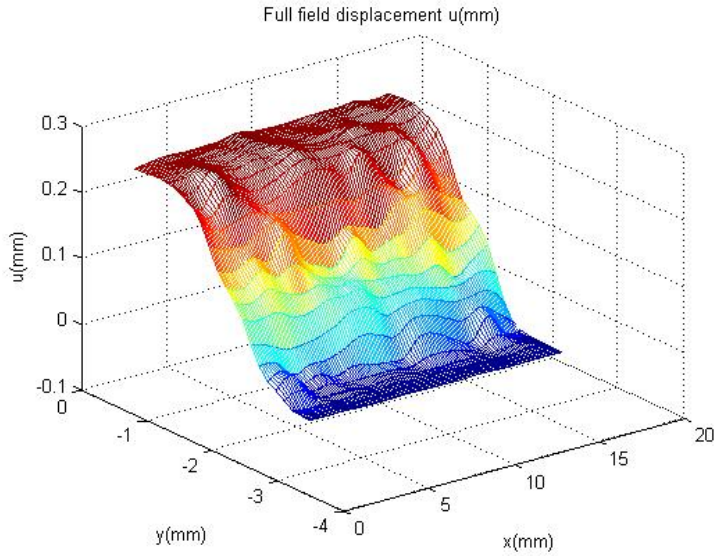

Figure 7. Full field displacement u(x,y), associated with x direction. 3D plot.

Taking the results of u(x,y) in three different position of x, i.e, x = 0.65 mm, x = 7.6 mm and x = 14.7 mm, it is possible to observe the linearity of curve u(x,y) versus y in the adhesive range, as shown in Fig. 8. It can also be observed that the adherends are underformated.

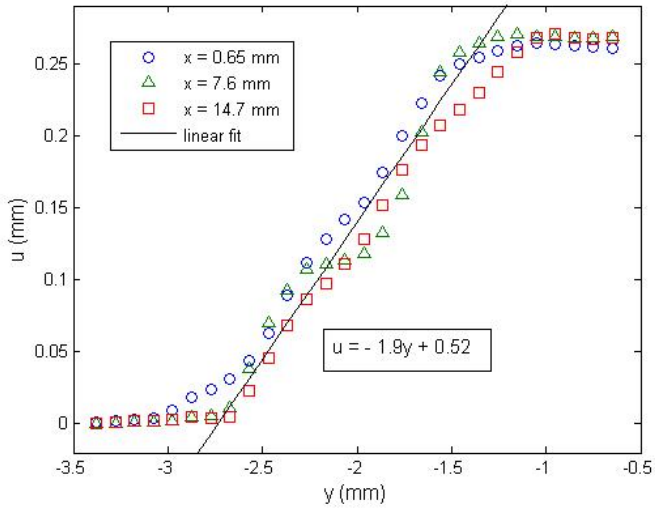

Figure 8. Displacement u(x,y)

Consequently, the shear deformation and stress represented by Eq. (2) and Eq. (3) can be taken into account without loss of generality. Thus, it is estimated the following results:

$$\gamma = \frac{\partial u}{\partial y} = 0.19 \text{ and } \tau = \gamma G_a = 47.5\,\text{kPa}$$

4.2. Numerical results

The Equation (9), knowing that the adherends have the same mechanical proprieties, can be rewritten as:

$$\tau(x) = \frac{P\omega}{2}\left[\frac{\cosh(\omega x)}{\sinh(\omega L/2)}\right] \tag{12}$$

Substituting the values considerate previously into Eq. (12), it is obtained the result present in Fig. 9. The shear stress is practically constant along axis x.

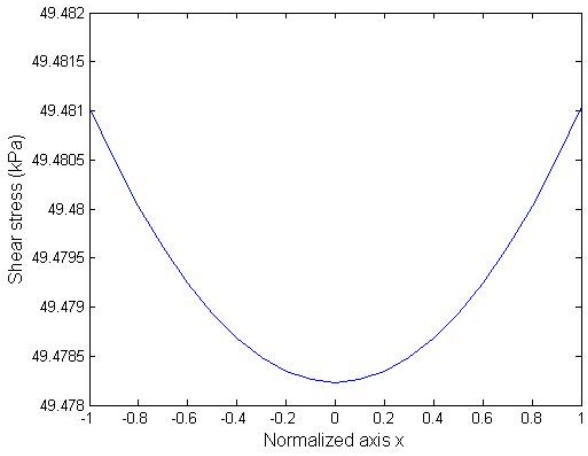

Figure 9. The shear stress

5. CONCLUTIONS

This is a preliminary work aimed at using experimental information obtained from Digital Image Correlation to analyze single lap joint. Digital Image Correlation was used to obtain the displacement field of specific regions. The results indicate good agreement between experimental and numerical analyses.

The main contribution of this work is to provide an experimental method of estimating the full field displacement and shear stress in a single lap joint. For future work the authors aim to approach the following problems: (i) estimate

the shear, normal and peel stress of bonded lap joints, considering the effect of the adherend bending and shear deformations; (ii) analyze fracture mechanics and singularities in bonded systems; (iii) estimate parameters of heterogeneous materials.

6. ACKNOWLEDGEMENTS

The authors would like to express their gratitude to the Ministry of Science and Technology through its research funding agency CNPq as well as to the LAA/UERJ for their help with development of the strain apparatus.

7. REFERENCES

Goland, M., Reissner, E., 1944. The stresses in cemented joints. Journal of Applied Mechanics 11, A17–A27.

D.A. Dillard, A.V. Pocius, Adhesion Science And Engineering – I , The Mechanics Of Adhesion, Elsevier Science B.V. First Edition 2002.

Quantian Luo, Liyong Tong, Fully-coupled nonlinear analysis of single lap adhesive joints, International Journal of Solids and Structures 44 (2007) 2349–2370

E. Oterkus , A. Barut , E. Madenci , S.S. Smeltzer III , D.R. Ambur, Bonded lap joints of composite laminates with tapered edges, International Journal of Solids and Structures 43 (2006) 1459–1489

L.C.S. Nunes, A. Castello, C.F. Matt and P.A.M. dos Santos, Parameter Estimation Using Digital Image Correlation and Inverse Problems, Solid Mechanics in Brazil 2007. 433-443.

8. RESPONSIBILITY NOTICE

The authors are the only responsible for the printed material included in this paper.